Theory, practice, and application of the van der Waals density functional

Ikutaro HAMADA
Department of Precision Engineering, Graduate School of Engineering, Osaka University
2-1 Yamadaoka, Suita, Osaka 565-0871, Japan

Abstract

The van der Waals density functional is a class of the density functional, which enables the description of the dispersion forces within the framework of density functional theory. In this article, theory and practice of the van der Waals density functional are reviewed, and applicability of a high-accuracy van der Waals density functional to various systems is demonstrated.

1 Introduction

Density functional theory (DFT) [1, 2] within the local density (LDA) and semilocal (GGA) approximations has been proven to be accurate in describing covalent, ionic, and metallic bondings, but has also been known to be unable to describe the dispersion forces (or often referred to as the van der Waals forces) [3] properly. This is because the dispersion forces originate from the instantaneous dipole-induced dipole interaction due to the electron fluctuation or the dynamic and nonlocal electron correlation, which are inherently missing in LDA and GGA. Wave function based theory and many body perturbation theory are shown to describe the dispersion interaction very accurately, but the computational cost is prohibitively large, hindering their application to complex systems, such as surfaces and interfaces.

There have been several proposals to correct the missing dispersion forces by adding the term proportional to $1/r^6$ (and higher-order terms) to the total energy within semilocal DFT, where r is the interatomic or inter-fragment distance. This type of approach was initiated in the field of the quantum chemistry (QC) [4], and has been established [5] and improved over the years by introducing accurate dispersion coefficients [6] and damping functions [7], as well as the environmental effects on the dispersion coefficients through the local electron density [8, 9] or coordination numbers [6]. Furthermore, accuracy of such pair-wise correction methods have been improved by introducing the three-body term[6] or the many-body dispersion[10]. See Refs. [11, 12, 13] for recent reviews.

The van der Waals density functional (vdW-DF) [14, 15, 16, 17, 18] is a versatile method that allows one to describe different interactions including the dispersion forces within the DFT framework. It is grounded on the electron gas tradition and the many-body perturbation theory as other constraint-based exchange-correlation (XC) functionals, and formally has no empirical or fitting parameters to reproduce the results of experiments or accurate theoretical calculations. The physical foundation of vdW-DF has been established [19], and theoretical and algorithmic improvements make it a method of choice in theoretical studies of materials and molecules.

In this article, I give a brief overview of the theory of vdW-DF and discuss a technical issue related to the use of pseudopotentials with applications. The Hartree atomic unit is used throughout unless otherwise specified.

2 Method

2.1 Theory

The XC energy, which is responsible for the quantum-mechanical electron-electron interaction, can be expressed exactly by using the adiabatic connection fluctuation dissipation theorem (ACFDT) [20, 21] as

$$E_{\rm xc} = -\int_0^1 \frac{d\lambda}{\lambda}\int_0^\infty \frac{du}{2\pi}{\rm tr}\left[\chi^\lambda(iu)V^\lambda\right] - E_{\rm self}, \tag{1}$$

where λ is the adiabatic parameter, which scales the electron-electron Coulomb interaction as $V^\lambda(\mathbf{r},\mathbf{r}') = \lambda/|\mathbf{r}-\mathbf{r}'|$, $\chi^\lambda(iu)$ is the reducible density-density response function at the adiabatic parameter λ and imaginary frequency $u = -i\omega$, and $E_{\rm self}$ is the electron-electorn self-energy defined by $E_{\rm self} = {\rm tr}\,[nV]$ with $V = V^{\lambda=1}$. Here, the trace is defined as ${\rm tr}[AB] = \iint d\mathbf{r}d\mathbf{r}' A(\mathbf{r},\mathbf{r}')B(\mathbf{r}',\mathbf{r})$ for arbitrary operators $\hat{A}$ and $\hat{B}$. $\chi^\lambda(\omega)$ is defined by $\delta n(\omega) = \chi^\lambda(\omega)\delta v_{\rm ext}(\omega)$, where $\delta n(\omega)$ and $\delta v_{\rm ext}(\omega)$ are the induced electron density and the external potential at the frequency ω, respectively.

The vdW-DF is constructed based on ACFDT as follows: $E_{\rm xc}$ may be split as

$$E_{\rm xc} = E_{\rm xc}^0 + E_{\rm c}^{\rm nl}, \tag{2}$$

where $E_{\rm xc}^0$ and $E_{\rm c}^{\rm nl}$ are the semilocal exchange-correlation and the nonlocal correlation energy functionals, respectively, and in vdW-DF, a tractable form of $E_{\rm c}^{\rm nl}$ has been developed based on several physical constraints.

We first introduce $\tilde{\chi}^\lambda$, which is defined by $\delta n(\omega) = \tilde{\chi}^\lambda(\omega)\delta V_{\rm scr}^\lambda(\omega)$ with $\delta V_{\rm scr}^\lambda(\omega)$ being the screened potential. $\chi^\lambda(\omega)$ and $\tilde{\chi}^\lambda(\omega)$ are related via the Dyson-like equation $\chi^\lambda = \tilde{\chi}^\lambda + \tilde{\chi}^\lambda V^\lambda \chi^\lambda$. Then, the full-potential approximation (FPA) is introduced, which sets $\tilde{\chi}^\lambda = \tilde{\chi}^{\lambda=1}$ and is exact at the van der Waals asymptote ($|\mathbf{r}-\mathbf{r}'| \to \infty$). This enables the analytic integration over λ and leads to $E_{\rm xc}$ in FPA as

$$E_{\rm xc} = \int_0^\infty \frac{du}{2\pi}{\rm tr}\left\{\ln\left[1-\tilde{\chi}^{\lambda=1}(iu)V\right]\right\} - E_{\rm self}. \tag{3}$$

This expression has a formal similarity with that obtained within the random phase approximation (RPA):

$$E_{\rm xc} = \int_0^\infty \frac{du}{2\pi}{\rm tr}\left\{\ln\left[1-\chi^0(iu)V\right]\right\} - E_{\rm self}, \tag{4}$$

where χ^0 is the irreducible density-density response function, which is connected to χ^λ via a Dyson equation $\chi^\lambda = \chi^0 + \chi^0 V^\lambda \chi^\lambda$ within RPA. $E_{\rm xc}$ within FPA can also be expressed as

$$E_{\rm xc} = \int_0^\infty \frac{du}{2\pi}{\rm tr}\left\{\ln\left[\nabla\cdot\varepsilon(iu)\nabla G\right]\right\} - E_{\rm self}, \tag{5}$$

where ε is the dielectric function and G is the Coulomb Green's function, i.e., $G = -4\pi V$.

To extract $E_{\rm c}^{\rm nl}$, $E_{\rm xc}^0$ is approximated with that of homogeneous electron gas within FPA, which is also called the internal XC energy, as

$$E_{\rm xc}^{\rm in} = \int_0^\infty \frac{du}{2\pi}{\rm tr}\left\{\ln\left[\varepsilon(iu)\right]\right\} - E_{\rm self}, \tag{6}$$

to obtain

$$E_{\rm c}^{\rm nl} = \int_0^\infty \frac{du}{2\pi}{\rm tr}\left\{\ln\left[\nabla\cdot\varepsilon(iu)\nabla G\right] - \ln\left[\varepsilon(iu)\right]\right\}. \tag{7}$$

It is apparent that by construction, $E_{\rm c}^{\rm nl}$ vanishes in the uniform electron-gas limit.

The thus obtained $E_{\rm c}^{\rm nl}$ is expanded in terms of a response function $S = \ln\varepsilon \approx 1-\varepsilon^{-1}$ up to the second order as

$$E_{\rm c}^{\rm nl} = \int_0^\infty \frac{du}{4\pi}{\rm tr}\left\{S^2(iu) - \left[\nabla S(iu)\cdot\nabla G\right]^2\right\} \tag{8}$$

and in the plane-wave representation as

$$E_{\rm c}^{\rm nl} = \int_0^\infty \frac{du}{2\pi}\int\frac{d\mathbf{q}}{(2\pi)^3}\int\frac{d\mathbf{q}'}{(2\pi)^3}\left[1-\left(\hat{q}\cdot\hat{q}'\right)^2\right] \times S_{\mathbf{q},\mathbf{q}'}(iu)S_{\mathbf{q}',\mathbf{q}}(iu), \tag{9}$$

where $\hat{q} = \mathbf{q}/|\mathbf{q}|$ and

$$\begin{aligned} S(\omega) &= S(\mathbf{r},\mathbf{r}',\omega) \\ &= \int\frac{d\mathbf{q}}{(2\pi)^3}\int\frac{d\mathbf{q}'}{(2\pi)^3}e^{-i\mathbf{q}\cdot\mathbf{r}}S_{\mathbf{q},\mathbf{q}'}(\omega)e^{i\mathbf{q}'\cdot\mathbf{r}'} \end{aligned} \tag{10}$$

This $E_{\rm c}^{\rm nl}$ is made tractable by applying the plasmon-pole approximation to $S_{\mathbf{q},\mathbf{q}'}(\omega)$, which is expressed as

$S_{\mathbf{q},\mathbf{q}'}(\omega) = \frac{1}{2}\left[\tilde{S}_{\mathbf{q},\mathbf{q}'}(\omega) + \tilde{S}_{-\mathbf{q},-\mathbf{q}'}(\omega)\right]$ and

$$\tilde{S}_{\mathbf{q},\mathbf{q}'}(\omega) = \int d\mathbf{r} e^{-i(\mathbf{q}-\mathbf{q}')\cdot\mathbf{r}} \times \frac{\omega_{\mathrm{p}}(\mathbf{r})}{[\omega + \omega_{\mathbf{q}}(\mathbf{r})]\left[-\omega + \omega_{\mathbf{q}'}(\mathbf{r})\right]}. \tag{11}$$

Here, $\omega_{\mathrm{p}}(\mathbf{r}) = 4\pi n(\mathbf{r})$ is the plasma frequency, where $n(\mathbf{r})$ is the electron density, and $\omega_{\mathbf{q}}(\mathbf{r})$ is the plasmon dispersion. The specific form of the response function S has been determined to satisfy the following constraints: (i) the time-reversal symmetry, (ii) the f-sum rule, (iii) cancellation of the self-energy, and (iv) charge conservation.

By writing the internal XC energy as

$$E_{\mathrm{xc}}^{\mathrm{in}} = \int d\mathbf{r} \epsilon_{\mathrm{xc}}^{\mathrm{in}}(\mathbf{r}) n(\mathbf{r}), \tag{12}$$

the internal XC energy per electron $\epsilon_{\mathrm{xc}}^{\mathrm{in}}$ reads

$$\epsilon_{\mathrm{xc}}^{\mathrm{in}}(\mathbf{r}) = \pi \int \frac{d\mathbf{q}}{(2\pi)^3}\left[\frac{1}{\omega_{\mathbf{q}}(\mathbf{r})} - \frac{2}{q^2}\right], \tag{13}$$

where $q = |\mathbf{q}|$ and the second term in the right-hand side is obtained by evaluating the self-energy term explicitly. The local plasmon dispersion is modeled by

$$\omega_{\mathbf{q}}(\mathbf{r}) = \frac{q^2}{2h[q/q_0(\mathbf{r})]} \tag{14}$$

with h being the switching function which controls the behavior of the plasmon depending on the wave vector and $q_0(\mathbf{r})$, an inverse length scale which depends on the electron density and its gradient $|\nabla n(\mathbf{r})|$. The functional form of h is determined in such a way that $\omega_{\mathbf{q}}(\mathbf{r})$ satisfies the small- and large-q cases (see below). By imposing

$$\int_0^\infty dy\,[h(y) - 1] = \frac{3}{4}, \tag{15}$$

q_0 is related to $\epsilon_{\mathrm{xc}}^{\mathrm{in}}$ as

$$\epsilon_{\mathrm{xc}}^{\mathrm{in}}(\mathbf{r}) = -\frac{3}{4\pi} q_0(\mathbf{r}). \tag{16}$$

In vdW-DF, $\epsilon_{\mathrm{xc}}^{\mathrm{in}}$ is made to be the GGA exchange plus LDA correlation functionals as

$$\epsilon_{\mathrm{xc}}^{\mathrm{in}}(\mathbf{r}) = F_{\mathrm{x}}^{\mathrm{in}}(s)\epsilon_{\mathrm{x}}^{\mathrm{LDA}}(\mathbf{r}) + \epsilon_{\mathrm{c}}^{\mathrm{LDA}}, \tag{17}$$

with the GGA exchange enhancement factor for the internal XC functional given by

$$F_{\mathrm{x}}^{\mathrm{in}}(s) = 1 - \frac{Z_{ab}}{9} s^2, \tag{18}$$

where $\epsilon_{\mathrm{x}}^{\mathrm{LDA}} = -3/4\pi k_{\mathrm{F}}$ with $k_{\mathrm{F}} = (3\pi^2 n)^{1/3}$ and $s = |\nabla n|/k_{\mathrm{F}} n$. By this choice, q_0 can be interpreted as k_{F} modulated by the energy ratio $\epsilon_{\mathrm{xc}}^{\mathrm{in}}/\epsilon_{\mathrm{x}}^{\mathrm{LDA}}$. In the first version of vdW-DF (vdW-DF1), $Z_{ab} = -0.8491$ based on the second-order gradient expansion for the slowly varying electron gas [22, 23], while in the second version of vdW-DF (vdW-DF2), $Z_{ab} = -1.887$ based on the second-order large-N expansion for the neutral atom [17].

The switching function h for the plasmon dispersion is determined to satisfy Eq. (15) and the following constraints. (i) $h(y) \approx \gamma y^2 + \cdots$ in the small-y limit, where γ is an arbitrary constant to ensure $h(0) = 0$, which corresponds to the charge conservation of the spherical XC hole model of the internal XC energy. (ii) $h(y) \to 1$ in the large-y limit, which corresponds to $\omega_{\mathbf{q}} \to q^2/2$ in the large q-limit. This constraint ensures the cancellation of the divergent term of E_{self} in the $q \to 0$ limit in $\epsilon_{\mathrm{xc}}^{\mathrm{in}}$. In Refs. [15, 17], the following form for h was used

$$h(y) = 1 - \exp(-\gamma y^2) \tag{19}$$

with $\gamma = 4\pi/9$, implying that the Gaussian form of the XC hole is used in $\epsilon_{\mathrm{xc}}^{\mathrm{in}}$ [19]. There is a freedom in the functional form of h and it is not limited to Eq. (19). Indeed, Berland *et al.* [24] proposed a functional form, which can improve the asymptotic behavior (and the so-called C_6 coefficient) of vdW-DF . To improve the accuracy of $E_{\mathrm{c}}^{\mathrm{nl}}$ as a part of the development of the third version of vdW-DF (vdW-DF3), Chakraborty *et al.* [25] proposed the following functional form

$$h(y) = 1 - \frac{1}{1 + \gamma y^2 + \gamma^2 y^4 + \alpha y^8}. \tag{20}$$

See Table 1 in Ref. [25] for the parameters γ and α. Note however, in the development of vdW-DF3, parameters in the functionals were optimized to the reference high-accuracy QC results of a large molecular data set. These parameters may vary when a plane-wave pseudopotential program is used in the optimization, depending on the pseudopotentials used.

After tedious but straightfoward calculations, one arrives at the following form of the nonlocal correlation functional

$$E_{\rm c}^{\rm nl} = \frac{1}{2}\iint drdr' n(\mathbf{r})\phi(d,d')n(\mathbf{r}'), \qquad (21)$$

where $d = q_0(\mathbf{r})|\mathbf{r}-\mathbf{r}'|$ and $d' = q_0(\mathbf{r}')|\mathbf{r}-\mathbf{r}'|$. The kernel function is given by

$$\begin{aligned}\phi(d,d') =& \frac{2}{\pi^2}\int_0^\infty daa^2 \int_0^\infty dbb^2 W(a,b) \\ & \times T[\nu(a),\nu(b),\nu'(a),\nu'(b)],\end{aligned} \qquad (22)$$

where

$$\begin{aligned}W(a,b) =& 2\big[(3-a^2)b\sin a\cos b \\ & + (3-b^2)a\cos a\sin b \\ & + (a^2+b^2-3)\sin a\sin b \\ & - 3ab\cos a\cos b\big]\end{aligned} \qquad (23)$$

and

$$\begin{aligned}T(w,x,y,z) =& \frac{1}{2}\left[\frac{1}{w+x}+\frac{1}{y+z}\right] \\ & \times\left[\frac{1}{(w+y)(x+z)}\right. \\ & \left.+\frac{1}{(w+z)(y+x)}\right],\end{aligned} \qquad (24)$$

with $\nu(y) = y^2/2h(y/d)$ and $\nu'(y) = y^2/2h(y/d')$ (d and d' are defined above). Calculating the ϕ on the fly is impractical, as the time-consuming double integral over the variables a and b is included. In practice, ϕ is calculated and tabulated in advance as a function of $D = (d+d')/2$ and $\delta = (d-d')/(d+d')$ ($0 \le D < \infty$ and $0 \le |\delta| < 1$) and the ϕ value is calculated on demand by interpolation. This approach works quite well, thank to the fact that ϕ is a smooth function of D and δ (See Fig. 1). Note that ϕ should be recalculated when different switching function h is employed, although the shapes of the h functions look similar, but $y^2/h(y)$, which is relevant to the plasmon dispersion, differs significantly [24, 25].

Remaining task in the development of vdW-DF is to determine the semilocal XC functional. Using $E_{\rm xc}^{\rm in}$ as $E_{\rm xc}^0$ is the most consistent approach within the framework of vdW-DF,

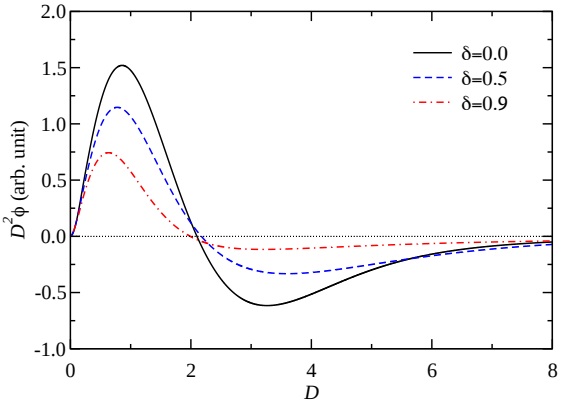

Figure 1: The kernel ϕ times D^2 as a function of D at various δ's obtained using an in-house kernel generation code [26].

but in practice, it results in less accurate results. By allowing crossover in the exchange functional and letting

$$E_{\rm xc}^0 = E_{\rm xc}^{\rm in} + \Delta E_{\rm x} = E_{\rm xc}^{\rm GGA} + E_{\rm c}^{\rm LDA}, \qquad (25)$$

the local correlation energy can be consistent with that of $E_{\rm xc}^{\rm in}$, and the semilocal exchange energy has been investigated.

In vdW-DF for layered materials [14] and general geometry vdW-DF (vdW-DF1) [15], the revised Perdew-Burke-Ernzherof (PBE) [27] exchange (revPBE) of Zhang and Yang [28] was employed because it does not show spurious binding of rare gas dimers from exchange only. However, it turns out that the revPBE exchange tends to overestimate the Pauli repulsion, leading to a too large separation between the fragments. In searching for more accurate exchange energy functional, Klimeš *et al.* [29] proposed a set of exchange functionals, leading to optPBE-vdW and optB88-vdW, based on the optimization to the reference QC results. Cooper [30] proposed an exchange functional (C09) which satisfies the following constraint: (i) The gradient expansion approximation (GEA) form in the slowly varying electron density (small-s) limit, i.e., $F_{\rm x}(s) = 1 + \mu s^2$ with $\mu = 0.0864$ [31], which is mainly responsible for the covalent interaction. (ii) The revPBE behavior in the homogeneous electron density (large-s) limit which is relevant to the vdW bonding. Although the μ value is not exactly the same as that of GEA for the slowly varying electron

gas ($\mu_{\rm GEA}$ = 10/81 [32]), this work demonstrated the importance of GEA in predicting accurate interaction energies and atomic geometries. Murray *et al.* [33] showed that the exchange enhancement factor should be proportional to $s^{2/5}$ in the large-s limit. They developed the revised PW86 [31] functional (PW86R), which obeys GEA in the small-s limit and has the $s^{2/5}$ behavior in the large-s limit for the exchange enhancement factor, and paired with a new $E_{\rm c}^{\rm nl}$, to propose vdW-DF2 [17]. Klimeš *et al.*[34] developed the optB86b exchange functional (and optB86b-vdW) in which the exchange enhancement factor obeys the gradient expansion approximation (GEA) in the slowly varying density (small-s) limit with $\mu_{\rm GEA}$ and has the $s^{2/5}$ behavior in the large s-limit. Berland and Hyldgaard [35] proposed an exchange functional (LV-PW86R), which is exactly the same as that of the internal exchange-correlation functional in the small-s region, while it reproduces the PW86R behavior in the large-s region. This semilocal exchange functional is the most consistent with that of the internal XC functional (consistent exchange), and thus the resulting vdW-DF functional is named vdW-DF-cx. Hamada [37] proposed an alternative one (B86R) based on the B86b [36] exchange functional, whose enhancement factor obeys GEA in the small-s limit and reproduces the original B86b behavior (proportional to $s^{2/5}$) in the large-s region. The B86R exchange is paired with $E_{\rm c}^{\rm nl}$ of vdW-DF2 and dubbed rev-vdW-DF2. In the latest development of vdW-DF (vdW-DF3) [25], B88 [38] and B86b [36] forms of the exchange enhancement factors are used. They are both designed to obey GEA in the small-s limit, and the remaining parameters are optimized to the reference QC results. The proposed GGA enhancement factors for vdW-DF are shown in Fig. 2, along with those for Perdew-Burke-Ernzerhof (PBE) [27] and PBEsol [39], the latter of which also obeys GEA in the slowly-varying density limit.

Although the precise performance of the vdW-DF functional depends on the combination of exchange and nonlocal correlation functionals, newly proposed functionals are shown to be more accurate than the original one,

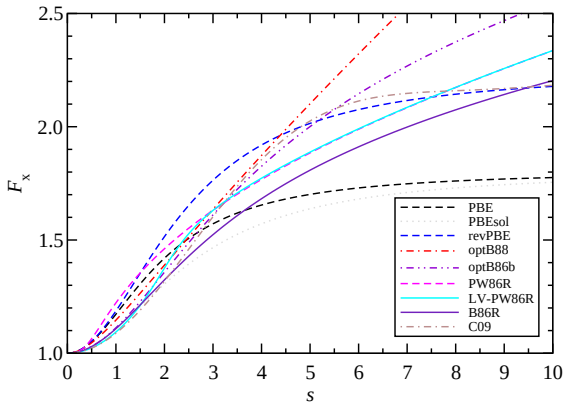

Figure 2: GGA enhancement factors ($F_{\rm x}$) proposed for various exchange-correlation functionals as a function of reduced density gradient (s).

and are versatile tools for accurate prediction of structures and energetics of materials, molecules, and interfaces. See Refs. [24, 25, 40, 41, 42, 43] for assessments of the different vdW-DF functionals on various materials and molecules.

2.2 Pseudopotentials

In electronic structure calculations, the pseudopotential and projector augmented wave (PAW) [44] methods are often used, in which (pseudo)potentials generated using certain XC functionals are used. As a rule of thumb, the XC functional used to generate pseudopotentials should be consistent with that for the calculations of materials and molecules, but this issue has not been discussed in vdW-DF calculations. This is presumably because the appropriate XC functionals for atomic systems have not known nor been discussed for the vdW-DF calculations. However, it should not be overlooked, given that the vdW-DF employs different exchange and nonlocal correlation functionals and is not a simple dispersion correction to a semilocal XC functional. Callsen and Hamada [45] proved that $E_{\rm c}^{\rm nl}$ vanishes in an isotropic system and showed that the XC functional to be used to generate (pseudo)potentials for specific vdW-DF functional is uniquely determined. For instance, the B86R exchange plus LDA correlation functional should be used to generate potentials

Table 1: vdW-DF functional and corresponding exchange and correlation functionals to be used in the atomic calculation and pseudo- and PAW-potential generation.

vdW-DF functional	exchange	correlation
vdW-DF1	revPBE	LDA
vdW-DF2	PW86R	LDA
optB88-vdW	optB88	LDA
optB86b-vdW	optB86b	LDA
vdW-DF^{C09_x}	C09	LDA
vdW-DF-cx	LV-PW86R	LDA
rev-vdW-DF2	B86R	LDA

for the rev-vdW-DF2 calculations of molecular/extended systems. See Table 1 for the exchange and correlation functionals to be used in the pseudo- and PAW-potential generation for vdW-DF calculations.

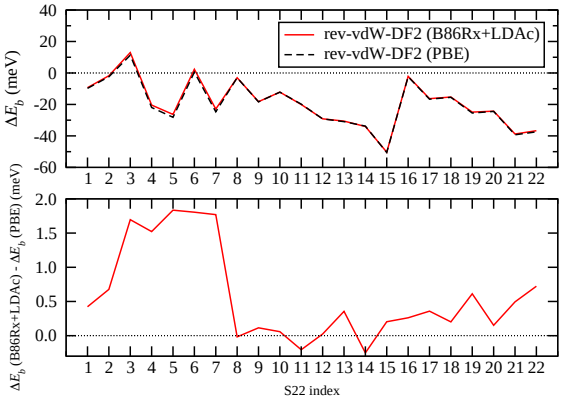

Figure 3: Deviations of the binding energies obtained using rev-vdW-DF2 with different PAW potentials with respect to the reference CCSD(T) results (ΔE_b, upper panel) and difference between the ΔE_b's obtained with different potentials (lower panel).

3 Application

In the following, applications of rev-vdW-DF2 to selected systems are presented. Emphasis is put onto the comparison of the results obtained using (psuedo)potentials generated with different XC functionals, i.e., the PBE and the B86R exchange plus LDA correlation (B86Rx+LDAc), the latter of which is compatible with rev-vdW-DF2. All the calculations were based on the PAW method and self-consistent vdW-DF as implemented [23, 46] in the QUANTUM-ESPRESSO [47] code. The proper extension of vdW-DF to the spin polarized system [48, 49] was adopted when necessary. The PAW potentials were generated using the input files supplied in the PSLIBRARY [50].

I first calculated the interaction energies for the S22 dataset [51], a set of 22 noncovalently bonded molecular duplexes. The calculations were performed at the S22 geometries [51] without any further optimization. Figure 3 depicts the deviations of the binding energies obtained using PBE and B86Rx+LDA potentials, with respect to the reference results obtained by the coupled cluster calculations with singlet, doublet, and perturbative triplet excitations [CCSD(T)] [52], along with the difference between the deviations obtained using different potentials. The binding energies obtained with PBE and B86Rx+LDA potentials are virtually the same (within the difference of 2 meV), and the mean absolute deviations are 20.5 and 20.8 meV for the former and the latter, respectively, validating the use of the PBE potentials in the vdW-DF calculations.

I then calculated the interlayer binding energy of graphite as a function of interlayer distance, as shown in Fig. 4. The equilibrium in-plane lattice constant is 2.46 Å, and interlayer distance and binding energy are 3.33 Å and 59.4 meV/atom, respectively, using both potentials. The interlayer binding energy is slightly overestimated as compared with quantum Monte-Carlo (56±5 meV/atom [53]), ACFDT-RPA (48 meV/atom [54]), and experiment (52±5 meV/atom [55]) but is in reasonable agreement with them.

I also performed the calculations of a benzene crystal. Figure 5 shows the binding energy of the benzene crystal in the *Pbca* symmetry as a function of the unit cell volume. The calculated equilibrium volume is 460 Å^3 with both potentials, and the binding energies are 532 and 531 meV/molecule with B86Rx+LDAc and PBE potentials, respectively, which are in reasonable agreement with the most recent experimental estimate of 573±23 meV/molecule [56]. Optimized cell parameters are a = 7.273 Å, b = 9.418 Å,

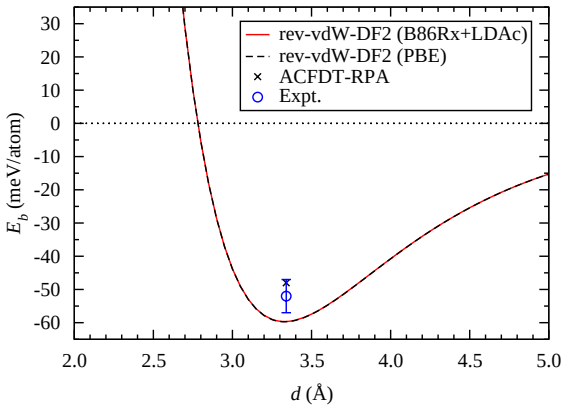

Figure 4: Binding energy of graphite (E_b) as a function of interlayer distance (d) using rev-vdW-DF2 with different potentials, along with the equilibrium energy and distance from ACFDT-RPA (Ref. [54]) and experiment (Ref. [55])

and $c = 6.723$ Å, which are also in reasonable agreement with the experimental values of $a = 7.36$ Å, $b = 9.37$ Å, and $c = 6.70$ Å [57].

These results suggest that the effect of using the potentials generated using the PBE functional is minor in vdW-DF calculations, at least with rev-vdW-DF2, although benchmark calculations on a larger set of materials and molecules need to be done.

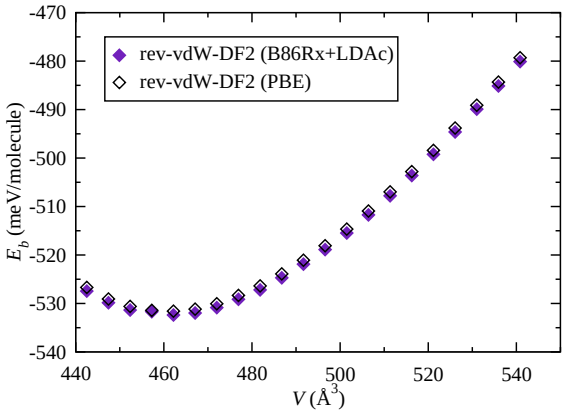

Figure 5: Binding energy of benzene crystal in the *Pbca* symmetry (E_b) as a function of unit cell volume (V) obtained using rev-vdW-DF2 and different potentials.

Finally, as a critical assessment of rev-vdW-DF2, I chose to calculate graphene adsorbed on Ni(111) in the atop-fcc configuration. In this calculation, B86Rx+LDAc potentials were

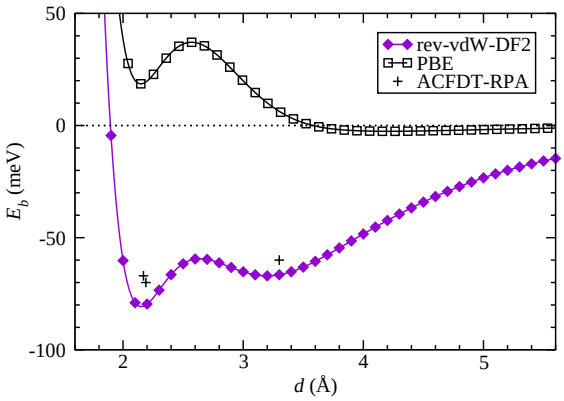

Figure 6: Binding energy of graphene on Ni(111) (E_b) as a function of distance from the surface (d) using rev-vdW-DF2 and PBE, along with the ACFDT-RPA results from Refs. [58, 59].

used but the result obtained using PBE potentials was found to be virtually identical. I also confirmed that present result is consistent with the one reported in Ref. [37] but with a different code. Figure. 6 shows the binding energy as a function of graphene-Ni surface distance by using PBE and rev-vdW-DF2 functionals (PBE potentials were used for the PBE calculations). It was found that the rev-vdW-DF2 slightly overestimates the binding energies, but is able to reproduce the binding energy curve with two local minima obtained using the ACFDT-RPA [58, 59], which is suggested to be a result of competing chemical and physical interactions. This demonstrates the accuracy of rev-vdW-DF2 in describing the adsorption system.

4 Summary

I give a brief review of the theory of vdW-DF, present recent theoretical advancements and some applications based on a variant of vdW-DF, rev-vdW-DF2. I discuss the proper choice of the XC functional to be used in the pseudo- and PAW-potential generation for vdW-DF calculations. It was found that the use of PBE potentials in rev-vdW-DF2 calculations has a minor impact on the calculated results, which may assure vdW-DF calculations in the literature. The accuracy of rev-

vdW-DF2 in describing the adsorption system is also demonstrated, and it is anticipated that its applicability is further broadened by introducing a fraction of the unscreened/screened Fock exchange, i.e., nonempirical hybrid vdW-DF [60, 61, 62].

Acknowledgements

The present work has been supported partly by Grants in Aid for Scientific Research on Innovative Areas "Hydrogenomics" (No. JP18H05519). Numerical calculations were in part performed using the super computers in Institute for Solid State Physics (ISSP), the University of Tokyo.

References

[1] P. Hohenberg and W. Kohn, Phys. Rev. **136**, B864 (1964).

[2] W. Kohn and L. J. Sham, Phys. Rev. **140**, A1133 (1965).

[3] F. London, Z. Physik **63**, 245 (1930).

[4] J. Hepburn, G. Scoles, and R. Penco, Chem. Phys. Lett. **36**, 451 (1975).

[5] S. Grimme, J. Comput. Chem. **27**, 1787 (2006).

[6] S. Grimme, J. Antony, S. Ehrlich, and H. Krieg, J. Chem. Phys. **132**, 154104 (2010).

[7] A. D. Becke and E. R. Johnson, J. Chem. Phys. **123**, 154101 (2005).

[8] A. Tkatchenko and M. Scheffler, Phys. Rev. Lett. **102**, 073005 (2009).

[9] T. Sato and H. Nakai, J. Chem. Phys. **131**, 224104 (2009).

[10] A. Tkatchenko, R. A. DiStasio, R. Car, and M. Scheffler, Phys. Rev. Lett. **108**, 236402 (2012).

[11] S. Grimme, A. Hansen, J. G. Brandenburg, and C. Bannwarth, Chem. Rev. **116**, 5105 (2016).

[12] J. Hermann, R. A. DiStasio, and A. Tkatchenko, Chem. Rev. **117**, 4714 (2017).

[13] E. Caldeweyher and J. G. Brandenburg, J. Phys. Condens. Matter **30**, 213001 (2018).

[14] H. Rydberg, *et al.*, Phys. Rev. Lett. **91**, 126402 (2003).

[15] M. Dion, *et al.*, Phys. Rev. Lett. **92**, 246401 (2004).

[16] M. Dion, *et al.*, Phys. Rev. Lett. **95**, 109902 (2005)

[17] K. Lee, *et al.*, Phys. Rev. B **82**, 081101 (2010).

[18] K. Berland, *et al.*, Rep. Prog. Phys. **78**, 066501 (2015).

[19] P. Hyldgaard, K. Berland and E. Schröder, Phys. Rev. B **90**, 075148 (2014).

[20] O. Gunnarsson and B. I. Lundqvist, Phys. Rev. B **13**, 4274 (1976).

[21] D. C. Langreth and J. P. Perdew, Phys. Rev. B **15**, 2884 (1977).

[22] D. C. Langreth and S. Vosko, Adv. Quantum Chem. **21**, 175 (1990).

[23] T. Thonhauser, *et al.*, Phys. Rev. B **76**, 125112 (2007).

[24] K. Berland, D. Chakraborty, and T. Thonhauser, Phys. Rev. B **99**, 195418 (2019).

[25] D. Chakraborty, K. Berland, and T. Thonhauser, J. Chem. Theory Comput. **16**, 5893 (2020).

[26] I. Hamada, vdwphi_drsll: A code to calculate the kernel function of the van der waals density functional, https://github.com/ikuhamada/vdwphi_drsll.

[27] J. P. Perdew, K. Burke, and M. Ernzerhof, Phys. Rev. Lett. **77**, 3865 (1996).

[28] Y. Zhang and W. Yang, Phys. Rev. Lett. **80**, 890 (1998).

[29] J. Klimeš, D. R. Bowler, and A. Michaelides, J. Phys. Condens. Matter **22**, 022201 (2009).

[30] V. R. Cooper, Phys. Rev. B **81**, 161104 (2010).

[31] J. P. Perdew and W. Yue, Phys. Rev. B **33**, 8800 (1986).

[32] P. R. Antoniewicz and L. Kleinman, Phys. Rev. B **31**, 6779 (1985).

[33] É. D. Murray, K. Lee, and D. C. Langreth, J. Chem. Theory Comput. **5**, 2754 (2009).

[34] J. Klimeš, D. R. Bowler, and A. Michaelides, Phys. Rev. B **83**, 195131 (2011).

[35] K. Berland and P. Hyldgaard, Phys. Rev. B **89**, 035412 (2014).

[36] A. D. Becke, J. Chem. Phys. **85**, 7184 (1986).

[37] I. Hamada, Phys. Rev. B **89**, 121103 (2014).

[38] A. D. Becke, Phys. Rev. A **38**, 3098 (1988).

[39] J. P. Perdew, *et al.*, Phys. Rev. Lett. **100**, 136406 (2008).

[40] T. Björkman, J. Chem. Phys. **141**, 074708 (2014).

[41] T. Rangel, *et al.*, Phys. Rev. B **93**, 115206 (2016).

[42] F. Tran, *et al.*, Phys. Rev. Materials **3**, 063602 (2019).

[43] S. Yanagisawa and I. Hamada in *Theoretical Chemistry for Advanced Nanomaterials: Functional Analysis by Computation and Experiment*, edited by T. Onishi (Springer Singapore, Singapore, 2020).

[44] P. E. Blöchl, Phys. Rev. B **50**, 17953 (1994).

[45] M. Callsen and I. Hamada, Phys. Rev. B **91**, 195103 (2015).

[46] R. Sabatini *et al.* J. Phys. Condens. Matter **24**, 424209 (2012).

[47] P. Giannozzi, *et al.* J. Phys. Condens. Matter **21**, 395502 (2009).

[48] T. Thonhauser, *et al.*, Phys. Rev. Lett. **115**, 136402 (2015).

[49] C. M. Frostenson, *et al.*, Electron. Struct. **4**, 014001 (2022).

[50] A. Dal Corso, Comput. Mater. Sci. **95**, 337 (2014).

[51] P. Jurečka, J. Sp̌oner, J. Cěrný, and P. Hobza, Phys. Chem. Chem. Phys. **8**, 1985 (2006).

[52] T. Takatani, *et al.*, J. Chem. Phys. **132**, 144104 (2010).

[53] L. Spanu, S. Sorella, and G. Galli, Phys. Rev. Lett. **103**, 196401 (2009).

[54] S. Lebégue, *et al.*, Phys. Rev. Lett. **105**, 196401 (2010).

[55] R. Zacharia, H. Ulbricht, and T. Hertel, Phys. Rev. B **69**, 155406 (2004).

[56] J. Yang, *et al.*, Science **345**, 640 (2014).

[57] W. David, R. Ibberson, G. Jeffrey, and J. Ruble, Physica B **180-181**, 597 (1992).

[58] F. Mittendorfer, *et al.*, Phys. Rev. B **84**, 201401 (2011).

[59] T. Olsen and K. S. Thygesen, Phys. Rev. B **87**, 075111 (2013).

[60] Y. Jiao, E. Schröder, and P. Hyldgaard, J. Chem. Phys. **148**, 194115 (2018).

[61] V. Shukla, Y. Jiao, C. M. Frostenson, P. Hyldgaard, J. Phys. Condens. Matter **34**, 025902 (2022).

[62] V. Shukla *et al.*, arXiv:2203.06682.